

Green Chemistry

Cutting-edge research for a greener sustainable future

Accepted Manuscript

View Article Online
View Journal

This article can be cited before page numbers have been issued, to do this please use: A. Sessa, S. Vllahu, P. Prete, I. Ritacco, L. Falivene, A. Carbone, G. Pierri, F. Rossi, I. Lagzi, M. Bastianini and R. Cucciniello, *Green Chem.*, 2026, DOI: 10.1039/D5GC05937B.



This is an Accepted Manuscript, which has been through the Royal Society of Chemistry peer review process and has been accepted for publication.

Accepted Manuscripts are published online shortly after acceptance, before technical editing, formatting and proof reading. Using this free service, authors can make their results available to the community, in citable form, before we publish the edited article. We will replace this Accepted Manuscript with the edited and formatted Advance Article as soon as it is available.

You can find more information about Accepted Manuscripts in the [Information for Authors](#).

Please note that technical editing may introduce minor changes to the text and/or graphics, which may alter content. The journal's standard [Terms & Conditions](#) and the [Ethical guidelines](#) still apply. In no event shall the Royal Society of Chemistry be held responsible for any errors or omissions in this Accepted Manuscript or any consequences arising from the use of any information it contains.

Green Foundation

View Article Online
DOI: 10.1039/D5GC05937B

1. This work explores the use of dimethyl carbonate for the preparation of advanced materials (ZIF-8) as safer alternatives to fossil-based DMF. The optimized reaction conditions allow ZIF-8 preparation with stoichiometric amounts of reagents (2-methylimidazole and Zn^{2+}), minimizing the need for a large excess of organic linker, as it is typically required in solvothermal methods with DMF or methanol.
2. Green metrics and the LCA methodology are used to assess the overall environmental impacts associated with the synthesis of ZIF-8 in different solvents. The results show that the dimethyl carbonate-based route for ZIF-8 preparation represents a promising and more sustainable alternative for ZIF-8 synthesis in comparison to DMF.
3. The results of this work open the way for the use of DMC in MOF preparation offering a viable and scalable alternative to conventional approaches based on toxic and non-renewable solvents.



Highly Efficient Synthesis of Microporous Zeolitic Imidazolate Framework-8 in Dimethyl Carbonate under Ambient Conditions

New Article Online
DOI: 10.1039/D5GC05937B

Alessandra Sessa,^{a,1} Sara Vllahu,^{a,1} Prisco Prete,^a Ida Ritacco,^a Laura Falivene,^a Alessia Carbone,^a Giovanni Pierri,^a Federico Rossi,^b Istvan Lagzi,^{c,d} Maria Bastianini,^e Raffaele Cucciniello^{a,*}

This work is dedicated to the memory of Prof. Roger Sheldon.

^a Department of Chemistry and Biology “Adolfo Zambelli”, University of Salerno, viale Giovanni Paolo II 132, 84084 Fisciano (SA), Italy.

^b Department of Physical Sciences, Earth and Environment, University of Siena, piazzetta Enzo Tiezzi 1, 53100 Siena, Italy.

^c Department of Physics, Institute of Physics, Budapest University of Technology and Economics, Műegyetem rkp. 3, H-1111 Budapest, Hungary

^d HUN-REN–BME Condensed Matter Physics Research Group, Budapest University of Technology and Economics, Műegyetem rkp. 3, H-1111 Budapest, Hungary

^e R&D Department, Prolabin&Tefarm S.r.l., 06134 Ponte Felcino - Perugia, Italy

¹ These authors contributed equally to this manuscript.



Abstract

In this work, we report the efficient synthesis of zeolitic imidazolate framework-8 (ZIF-8) under ambient conditions in only 1 h, using a slightly polar solvent, dimethyl carbonate (DMC), one of the recommended green solvents according to the CHEM21 solvent selection guide. The optimized reaction conditions allow ZIF-8 preparation with stoichiometric amounts of reagents (2-methylimidazole and Zn^{2+}), minimizing the need for a large excess of organic linker, as it is typically required in solvothermal methods with DMF, methanol, or water. These results demonstrate that ZIF-8 can be successfully prepared even in slightly polar media, in contrast to previous literature. Yields ranging from 80 to 98% were obtained, and the influence of the solvent on the reaction was systematically discussed. The resulting ZIF-8 was fully characterized, revealing microporous materials with excellent textural properties and among the highest reported specific surface areas (up to $1708 \text{ m}^2 \text{ g}^{-1}$) and pore volumes (up to 0.83 cc g^{-1}), compared to state-of-the-art materials. In addition, DMC was efficiently recycled over three consecutive cycles, maintaining high yields and preserving the crystallinity of ZIF-8. The sustainability of the proposed method was thoroughly evaluated using both green metrics (E-factor and PMI) and Life Cycle Assessment (LCA) confirming a significant reduction in environmental impacts compared to the most commonly used organic solvent, for this purpose, dimethylformamide (DMF).



Introduction

View Article Online
DOI: 10.1039/D5GC05937B

Zeolitic imidazolate frameworks (ZIFs) are a subclass of the well-known metal–organic frameworks (MOFs), a kind of crystalline porous materials consisting of metal cations coordinating organic ligands. In particular, the M-Im-M fragment in ZIFs, where M is the metal ion and Im is an imidazolate linker, features a bond angle of approximately 145° , closely matching the preferred angle of the Si-O-Si bond in many zeolites.^{1,2} The defining feature of ZIFs is their inherent tunability, and by varying metal ions and organic linkers, it is possible to design frameworks with tailored pore sizes, shapes, and surface functionalities, adapting the material to specific needs.^{3,4} These materials have gained increasing interest among the scientific community for their extensive structural design possibilities. Among them, ZIF-8 stands out, consisting of tetrahedral units where each Zn^{2+} ion coordinates four 2-methylimidazolate (Hmim) linkers, forming a three-dimensional sodalite (SOD)-type topology. The resulting structure features uniform micropores with internal cavities of approximately 1.16 nm pore diameter, which are interconnected through small six-membered windows of 0.34 nm.^{5,6} Due to their remarkable properties such as high crystallinity and porosity, large specific surface area, and exceptional thermal and chemical stability, ZIF-8 is considered an attractive candidate for various applications, including catalysis, gas storage and separation, drug delivery, and chemical sensing.^{7–13} The properties of ZIF-8 are strongly influenced by synthesis methods and parameters, such as temperature, pH, reaction time, solvent, reactants' molar ratio, and concentration. In this respect, many efforts have been made to control the structural and morphological properties of ZIF-8 through the synthetic process. The solvothermal method using N,N-dimethylformamide (DMF) as solvent is commonly employed for the traditional synthesis of ZIF-8, first introduced by Park *et al.*¹⁴ Reports using DMF under solvothermal conditions (140 °C for 24 h), obtained highly crystalline ZIF-8 with BET specific surface area of over $1300 \text{ m}^2 \text{ g}^{-1}$ and pore volume of $0.51 \text{ cm}^3/\text{g}$, though with moderate yields ($\sim 30\%$).^{15,16} However, since DMF is a toxic, fossil-based solvent that poses risks to human health and to the environment,¹⁷ developing new synthetic processes that use alternative solvents has become a primary goal in this field. Methanol (MeOH) was proposed as the first alternative to DMF. Cravillon *et al.* successfully synthesized ZIF-8 at room temperature using MeOH, achieving crystalline materials with 23% yield.

Methanol is advantageous for its lower toxicity compared to DMF, lower boiling point and good solubilizing ability. However, the relatively low yields, together with the fact that MeOH molecules can be trapped in the ZIF-8 micropores due to their size being close to the [SOD] window diameter (0.34 nm), may cause structural defects or hinder pore accessibility.¹⁶

As a safer alternative, water was also tested. As a matter of fact, Kida *et al.* reported the synthesis of ZIF-8 in water at room temperature by carefully optimizing the metal-to-ligand ratio and pH. The use of a high excess of Hmim (e.g., $\text{Zn}^{2+}:2\text{-mIm} = 1:60$ or higher) enabled the formation of highly crystalline ZIF-8 with yields up to 94.2% in 1h. However, such large excesses of ligand generate considerable reagent waste. Additionally, water-based syntheses often require a strongly alkaline environment to ensure an efficient deprotonation of the linker and avoid hydrolysis of Zn^{2+} . Even slight variations in pH, temperature, or concentration can drastically affect morphology, particle size, and phase purity.^{18–20} Partial control over these factors has been achieved through diffusion-assisted MOF production, particularly when a gel phase is employed in aqueous media or water/DMF mixtures.^{21–25}

Glycerol carbonate (GlyC) has been successfully tested for the first time as a green solvent^{26,27} for the synthesis of ZIF-8, showing a comparable performance to DMF. Using GlyC, mesoporous ZIF-8 was obtained with a pore volume of $0.58 \text{ cm}^3 \text{ g}^{-1}$ and $660 \text{ m}^2 \text{ g}^{-1}$ as the BET specific surface area. These results highlighted the role of the solvent on the ZIF-8 characteristics, opening the way to a relevant research area in this context. As a matter of fact, a high-viscosity ($\eta (T = 298.15 \text{ K}) = 0.0854 \text{ Pa s}$) and a high-boiling point (627.05 K) polar and protic solvent, as in the case of GlyC,²⁸ favors the



development of mesoporous material, as obtained instead through different synthetic approaches.²⁹ In Table 1 are reported the optimized reaction conditions for the ZIF-8 preparation in the aforementioned solvents. DOI: 10.1039/D5GC05937B

Table 1. Relevant results of solvo(hydro)thermal preparation of ZIF-8 in different solvents.

Synthesis method	Molar ratio Zn ²⁺ /2-mIm	[Zn ²⁺] (M)	[Hmim] (M)	<i>T</i> (°C)	<i>t</i> (h)	Yield %	BET Specific Surface Area (m ² g ⁻¹)	Pore volume (cc g ⁻¹)
Solvothermal (DMF) ¹⁶	1/8	0.2	1.6	140	24	30	1370	0.51
Solvothermal (MeOH) ³⁰	1/8	0.02	0.2	RT	24	23	1549	0.59
Hydrothermal (H ₂ O) ³¹	1/60	0.03	1.5	RT	1	94	1550	0.68
Solvothermal (GlyC + NaOH) ²⁷	1/2	0.01	0.02	100	24	57	660	0.58

In conclusion, these synthetic routes rely on polar protic or aprotic solvents, which facilitate linker deprotonation and stabilize coordination intermediates. However, the need for excess reagents or post-synthesis treatments highlights the lack of an ideal balance between process efficiency and environmental impact. In the solvothermal method, the solvent plays a crucial role. It governs not only reagent solubility and diffusion but also coordination dynamics, nucleation rates, and crystal growth.^{16,32} Rather than focusing on each individual property, it is the combination of features, such as polarity, viscosity, boiling point, and surface tension, that determines solvent effectiveness. An ideal solvent should provide adequate solubility for all reagents, promote homogeneous mixing, and not interfere with the coordination environment of the metal and linker. Based on these criteria, optimal solvents are typically polar enough to dissolve precursors, yet with a moderate dielectric constant and low reactivity to avoid disrupting the coordination mechanism. A relatively high boiling point can support stable reaction conditions and easier handling during solvent recovery.^{33,34}

Among organic carbonates (OCs), dimethyl carbonate (DMC) is one of the most versatile and recommended examples by ACS CHEM21 solvent selection guide.^{35,36} With its low dielectric constant, viscosity and boiling point (~90 °C) combined with high vapor pressure, DMC is easy to handle, recover and remove from reaction media, improving process efficiency.³⁷ It is non-toxic, readily biodegradable in atmosphere (90% within 28 days), and exhibits low (eco)toxicity without irritating or mutagenic effects. Owing to this excellent physicochemical and safety profile, DMC is increasingly used as a green alternative to fossil-based and dipolar aprotic solvents (e.g., MEK, NMP, DMSO, EtOAc) in several applications. Moreover, its potential production from methanol and CO₂, in line with Green Chemistry principles, could enhance its relevance as a benchmark solvent for environmentally responsible processes.^{38,39}

In this work, we investigated the preparation of ZIF-8 in a weakly polar solvent, dimethyl carbonate (DMC). The main goal of this study was to explore the feasibility of ZIF-8 synthesis in slightly polar media in order to establish a new synthetic approach, comparing the properties of the resulting materials with those previously reported in literature.

This work could also provide new insights into the use of DMC–MeOH mixtures. These mixtures are generally obtained after the methylation reaction in the presence of DMC as the methylating agent, and they are usually either disposed of or separated by azeotropic distillation.⁴⁰ In this regard, a recent life cycle assessment on the production of 1 g of ZIF-8 in glycerol carbonate highlighted the predominant impact of the solvent preparation, which could be partially reduced by valorizing

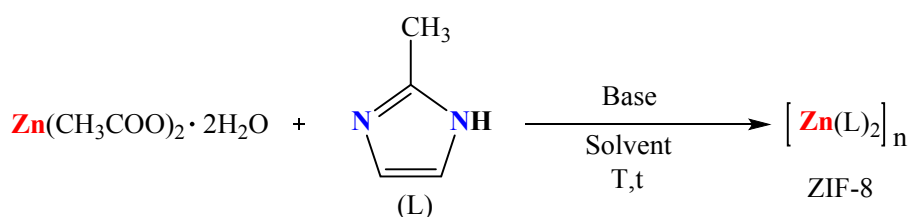


precisely the DMC-MeOH mixture generated as byproduct during its synthesis (glycerol transcarboxylation with DMC).⁴¹ Thus, following a circular economy approach, we adopted the ambitious idea of using them as solvent media for ZIF-8 preparation to broaden the scope of our evaluation.

In addition, the recyclability of DMC was investigated over multiple syntheses and a proper sustainability assessment was provided through green metrics (E-factor and PMI) and a comparative LCA with the same reaction carried out in DMF, the most commonly used organic solvent for ZIF-8 preparation.

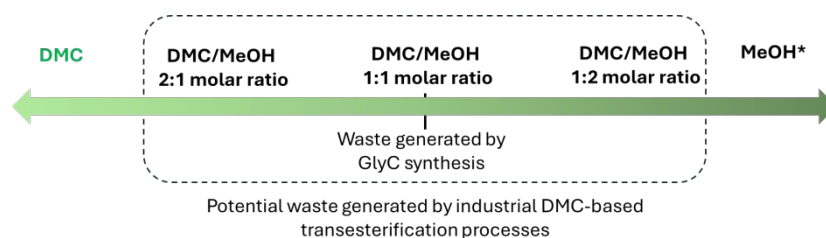
Results and discussion

We employed pure DMC and DMC/MeOH mixtures as solvents for ZIF-8 synthesis. The synthesis was carried out using zinc acetate dihydrate ($\text{Zn}(\text{OAc})_2 \cdot 2\text{H}_2\text{O}$) as the Zn^{2+} source and Hmim in the presence of NaOH as a base, under continuous stirring (see Scheme 1, where (L)=Hmim).



Scheme 1. ZIF-8 synthesis.

Starting from pure DMC, the DMC/MeOH 1:1 molar ratio—actually obtained as a by-product in the synthesis of GlyC via glycerol transcarboxylation with DMC⁴²—along with additional compositions such as 2:1 and 1:2 DMC/MeOH, were also explored to extend the scope of this work (see Scheme 2). Syntheses carried out in methanol were not investigated (MeOH* in Scheme 2), as they have already been extensively reported in the literature.^{30,43}



Scheme 2. Schematic representation of solvents employed for ZIF-8 synthesis.

For all systems, various reaction conditions (solvent, temperature (25 °C and 60 °C), time (1 h), metal-to-ligand molar ratio, [metal] and [ligand] concentrations, and [base]) were systematically investigated (see Table S2) to assess their influence on the resulting ZIF-8 materials.

Considering the previous literature, the formation of ZIF-8 begins with the coordination of anhydrate Hmim molecules to Zn^{2+} ions. This interaction produces the $[\text{Zn}(\text{2-Hmim})_2]^{2+}$ complex, which then undergoes successive deprotonation steps and further coordination with Zn^{2+} ions, ultimately leading to the growth of ZIF-8 crystals. Throughout this process, both 2-Hmim and OH^- ions can participate in the deprotonation of the $[\text{Zn}(\text{2-Hmim})_2]^{2+}$ complex, underlining the key influence of their relative concentrations on the crystallization pathway. When the amount of 2-Hmim is insufficient, leaf-like structures with low specific surface area are obtained instead of the desired dodecahedral ZIF-8 crystals.⁴⁴

The obtained products were characterized using several techniques, and the full characterization is reported in the Supporting Information (SI). According to observed X-ray powder diffraction (XRPD)



peaks and their comparison with reference data from the Cambridge Crystallographic Data Centre (CCDC), pure ZIF-8 phase was obtained under optimized reaction conditions, depending on the solvent (Figure 1a, 2a and 2d). Both the synthesized samples in DMC and DMC/MeOH mixtures were characterized by means of XRPD analysis showing the main characteristic diffraction peaks of ZIF-8 that were indexed in the range of 5° - 30° to 7.3° (110), 10.4° (200), 12.7° (211), 14.7° (220), 16.4° (310) and 18.0° (222) (see SI for the full characterizations).

An interesting finding concerns the use of stoichiometric amounts of Hmim and Zn^{2+} to generate ZIF-8 (Table 2-3). In fact, in the vast majority of cases reported in the literature, the amount of Hmim is greater than the stoichiometric ratio ($Hmim:Zn^{2+} = 2:1$).^{16,45} To date, the synthesis of ZIF-8 with a stoichiometric ratio of reactants has been achieved only by using either a large excess of base or a jet-mixer reactor^{46,47} or in the presence of a cyclic organic carbonate as GlyC.²⁷

To optimize the use of a base and the $Zn^{2+}/Hmim$ molar ratio for ZIF-8 preparation, we carried out systematic experiments in the DMC:MeOH 2:1 mixture (see data in Table 2).

We observed excellent reaction yields in the presence of stoichiometric amounts of base relative to Hmim. These conditions were then applied to other solvents. As mentioned earlier, the presence of a base promotes the deprotonation of the $[Zn(2-mIm)_2]^{2+}$ complex, facilitating ZIF-8 formation. The data also confirmed that ZIF-8 forms at $25^{\circ}C$ only in the presence of 5 mM Zn^{2+} and 10 mM Hmim. At higher reagent concentrations (10:20 mM and 20:40 mM), ZIF-8 formation requires higher temperatures to overcome kinetic barriers and enable the growth of well-ordered ZIF crystals, rather than alternative polymorphs.⁴⁸

Table 2. Effect of base and $Zn^{2+}/Hmim$ molar ratio on the ZIF-8 preparation in DMC/MeOH 2:1 mixture.

Entry	$[Zn^{2+}]$ (mM)	$[Hmim]$ (mM)	C_{NaOH} (mM)	Solvent	V_{TOT} (solution) (mL)	T ($^{\circ}C$)	t (h)	ZIF-8 [a]	Yield (%)	BET SSA ($m^2 g^{-1}$)	Total pore volume ($cc g^{-1}$)
1	20	40	10	DMC/MeOH (2:1)	50	60	1	✓	51.1	1580	0.60
2	20	40	10	DMC/MeOH (2:1)	50	RT	1	✗	-	-	-
3	10	20	10	DMC/MeOH (2:1)	50	60	1	✓	41.8	1235	0.63
4	10	20	10	DMC/MeOH (2:1)	50	RT	1	✗	-	-	-
5	10	20	20	DMC/MeOH (2:1)	50	60	1	✓	97.2	770	0.32
6	10	20	20	DMC/MeOH (2:1)	50	RT	1	✗	-	-	-
7	5	10	10	DMC/MeOH (2:1)	100	60	1	✓	97.5	921	0.38
8	5	10	10	DMC/MeOH (2:1)	100	RT	1	✓	86.2	1350	0.51

Considering the results, we adopted the optimized reaction conditions for further experiments ($[Zn^{2+}] = 5$ mM; $[Hmim] = 10$ mM; $[NaOH] = 10$ mM).

Table 3 reports the subsequent results in DMC/MeOH (1:1 and 1:2) and pure DMC, highlighting the critical role of reaction conditions in obtaining ZIF-8, which vary depending on the solvent used. This observation is consistent with previous studies in other solvents.^{1,16,27}

Table 3. ZIF-8 preparation in DMC and DMC/MeOH (1:1 and 1:2) mixtures.



Entry	[Zn ²⁺] (mM)	[Hmim] (mM)	C _{NaOH} (mM)	Solvent	V _{TOT} (solution) (mL)	T (°C)	t (h)	ZIF- 8 [a]	Yield (%)	BET SSA (m ² g ⁻¹)	Total pore volume (cc g ⁻¹)
9	5	10	10	DMC/MeOH (1:1)	100	60	1	✓	69.5	1147	0.51
10	5	10	10	DMC/MeOH (1:1)	100	RT	1	✗	-	-	-
11	5	10	10	DMC/MeOH (1:2)	100	60	1	✗	-	-	-
12	5	10	10	DMC/MeOH (1:2)	100	RT	1	✗	-	-	-
15	5	10	10	DMC	100	60	1	✗	-	-	-
16	5	10	10	DMC	100	RT	1	✓	91.3	1522	0.75

As highlighted in Tables 2-3, high ZIF-8 yields above 90% were obtained in pure DMC, in contrast to the values generally reported for organic solvents such as DMF, methanol or GlyC, where yields are typically below 50%.^{16,27,30,31} Results obtained in DMC:MeOH 1:1 and 2:1 mixtures further demonstrate the possibility of using solvent mixtures in addition to pure DMC. In particular, the DMC:MeOH 2:1 mixture yielded 97.5% (see entry 7 in Table 2), among the highest reported in this field. This improvement is attributed to the presence of methanol, which increases the polarity of the reaction medium, enhancing ion diffusion and promoting nuclei aggregation.

In DMC, no ZIF-8 formation was observed at higher temperatures (60 °C) after 1 h, despite successful crystallization at ambient temperature. This behavior can be attributed to the limited ability of DMC to dissolve polar compounds such as Hmim and the zinc salt, and this limitation becomes more pronounced at elevated temperatures. Furthermore, higher temperatures accelerate aggregation kinetics, hindering the proper organization into ZIF-8 frameworks. The low viscosity of DMC also promotes uncontrolled diffusion, further limiting ZIF-8 formation. In contrast, at room temperature, the reaction proceeds more slowly, favoring the formation of stable nuclei.

Moreover, in DMC we obtained crystalline ZIF-8 with a high specific surface area (1522 m² g⁻¹) in only 1 h, as well as a total pore volume of 0.75 cc g⁻¹. The material is characterized by a narrow and sharp PSD centered around 0.588 nm half pore width, consistent with the expected ZIF-8 pore size.¹⁶

The adsorption isotherms (Figures 1 and 2, panels b,e) show a steep increase in nitrogen uptake at low relative pressures ($P/P_0 < 0.05$), characteristic of microporous materials (pore radius < 10 Å) and reflecting the rapid filling of the ZIF-8 framework.⁴⁹ At higher relative pressures, the isotherms follow a slight gradual increase in adsorption and a minor hysteresis loop at $P/P_0 \approx 0.4-0.9$. According to the IUPAC classification, this adsorption behavior can be associated with a combination of Type I and Type IV isotherms with a H4-type hysteresis, suggesting a predominantly microporous structure with a minor mesoporous contribution.^{50,51}

When combining the isotherms with the corresponding pore size distributions, differences between the samples can be observed. In the case of ZIF-8 synthesized in DMC (Figure 1c), the PSD shows a predominant microporous contribution (5–10 Å), together with a minor peak in the initial mesopore range (10–50 Å), indicating the coexistence of micro- and mesoporosity.^{51,52} Despite a similar adsorption behavior, no significant mesoporous contribution is observed in the PSD of samples synthesized in DMC/MeOH mixtures (Figures 2c and 2f). This slight deviation from an ideal Type I profile and the presence of hysteresis can be attributed to a mesoporosity arising from particle aggregation,⁵³ as also supported by SEM analysis.



The concentration of ZIF-8 precursors also plays a key role. In DMC, ZIF-8 formation was observed using stoichiometric amounts of reagents at lower concentrations (5 mM Zn^{2+} and 10 mM Hmim) compared to the more polar DMC/MeOH 2:1 mixture, where higher concentrations (10:20 mM and 20:40 mM) also favored ZIF-8 formation. This behavior is due to the limited solubility of the precursors in DMC, which restricts the use of more concentrated solutions. Indeed, in pure DMC, using 10 mM Zn^{2+} and 20 mM Hmim, no ZIF-8 formation was observed at either 25 °C or 60 °C after 1 h.

In a DMC:MeOH 1:2 mixture, ZIF-8 formation was not observed, whereas under the same optimized conditions in a DMC:MeOH 2:1 solvent system, the synthesis proceeded successfully. This behavior is consistent with literature reports,⁵⁴ where changes in solvent composition often necessitate re-optimization of reaction parameters. The higher methanol content shifts the solvent properties closer to those of pure methanol, for which different conditions are required, such as a large excess of the organic linker or longer reaction times.

Figures 1 and 2 report the characterization of ZIF-8 samples obtained in DMC and DMC:MeOH mixtures of 2:1 and 1:1 molar ratio.

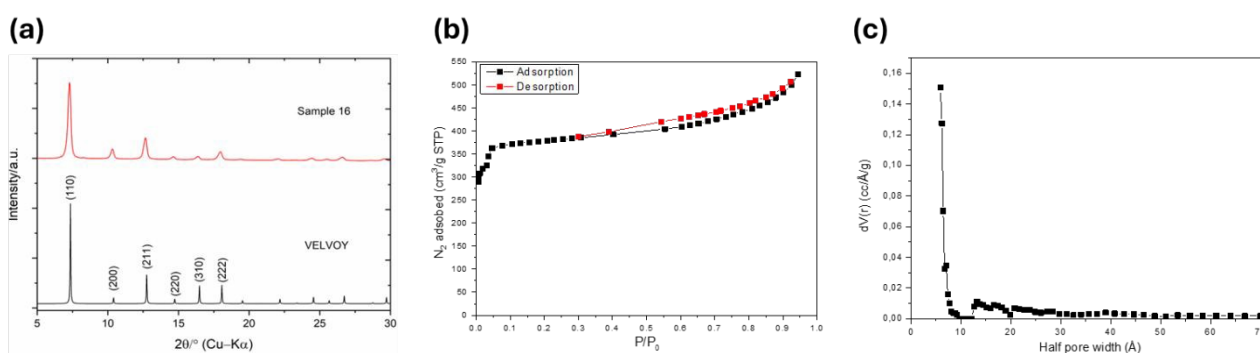


Figure 1. (a) Comparison between the XRPD experimental diffraction pattern (red) and calculated diffraction pattern (black, CCDC code VELVOY).⁵⁵ (b) N_2 adsorption/desorption isotherm and (c) NLDFT pore size distribution of ZIF-8 crystals obtained in DMC.

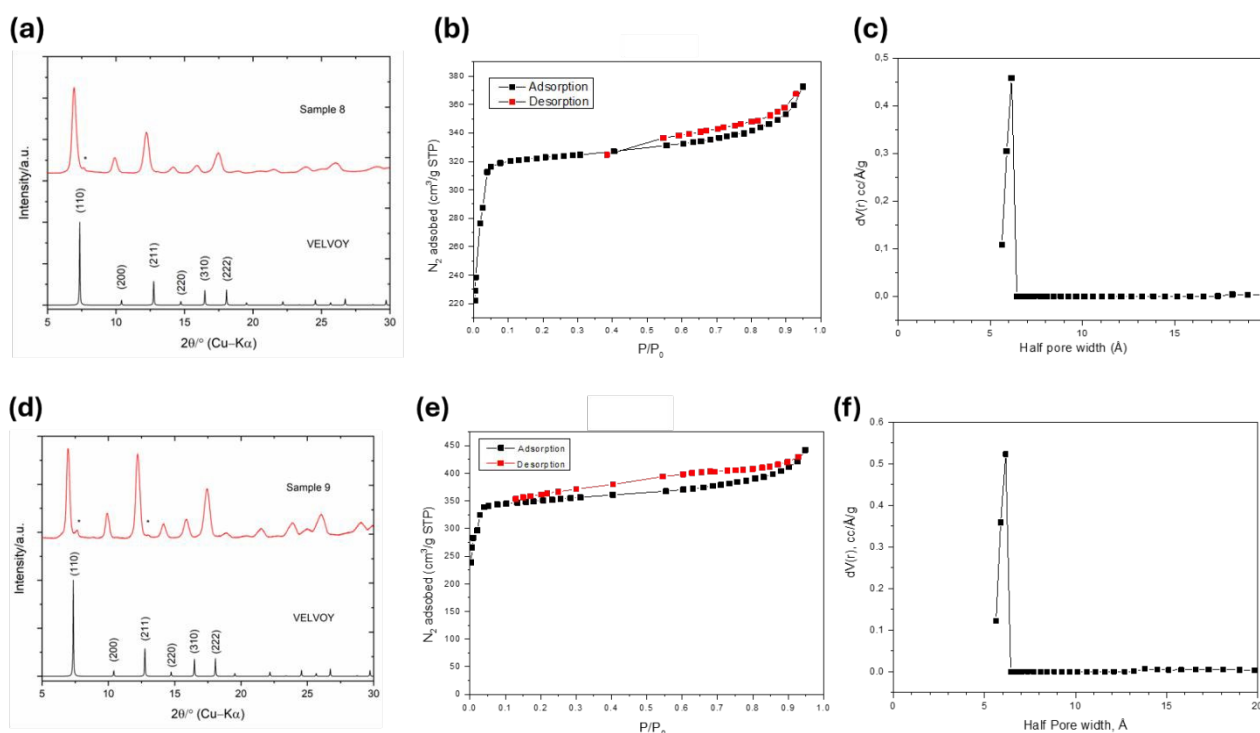
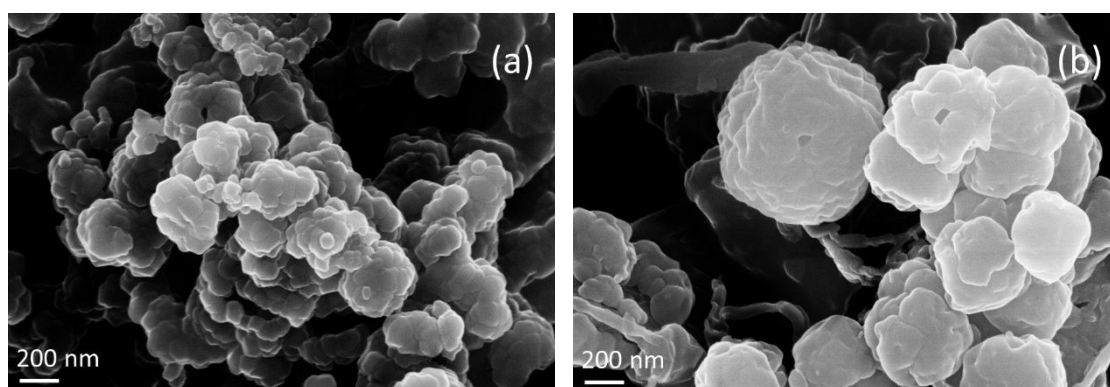


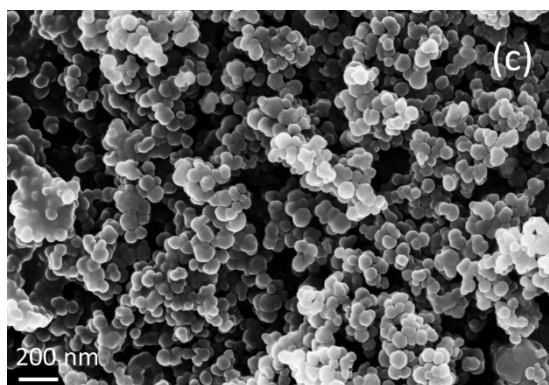
Figure 2. ZIF-8 crystals prepared in DMC/MeOH mixtures: (a-c) 2:1 and (d-f) 1:1 molar ratios. (a,d) Comparison between the XRPD experimental diffraction pattern (red) and calculated diffraction pattern (black, CCDC code VELVOY). The diffraction peaks belonging to impurities are marked with *. (b,e) N₂ adsorption/desorption isotherm and (c,f) NLDFT pore size distribution.

In addition to the previously discussed results, Figure S7 (section S5.2 in SI) clearly highlights the high thermal stability of the obtained ZIF-8. To simplify the discussion, we reported one representative sample for each solvent/mixture. All samples exhibited comparable thermal behavior with an excellent thermal stability up to 350-380 °C. Specifically, samples prepared in DMC:MeOH 2:1 (entry 8 in Table 2) and in DMC:MeOH 1:1 mixture (entry 9 in Table 3) showed two distinct weight losses: an initial minor loss of approximately 1-2% below 352 °C and 367 °C, respectively, due to trace adsorption of atmospheric humidity in the micropores of ZIF-8 during the sample preparation. The latter is in agreement with the work reported by Kim et al.³² In addition, we observed a second major and gradual degradation up to 800 °C, associated with the thermal decomposition of the organic fraction. ZIF-8 prepared in pure DMC (entry 16 in Table 3), on the other hand, exhibited a single and remarkable weight loss observed in the range 380-800 °C.

In all cases, framework degradation started occurring between 350 °C and 380 °C, confirming the structure integrity and high thermal stability of the ZIF-8 samples synthesized in this study, in agreement with literature data for analogous materials.^{4,56-58}

SEM micrographs of selected samples have also been reported in Figure 3. SEM images highlight the strong polydispersity of the synthesized ZIF-8 samples. The material consists of aggregates of sub-spherical nanoparticles with poorly defined facets, alongside larger and more regular crystallites, some showing the typical truncated rhombic dodecahedral morphology. The coexistence of ultrafine nuclei, grown particles, and aggregates spanning from <50 nm to >200 nm confirms a broad size distribution resulting from simultaneous rapid nucleation and subsequent crystal growth.⁵⁹ In line with previous study we observed polydispersity associated with stirring as well as the nanoparticle size broad distribution in the presence of organic solvents.⁵⁹ The morphological discrepancies between the samples can be mainly attributed to solvent composition (DMC vs DMC/MeOH mixtures), temperature effects⁶⁰ (higher temperatures modify nucleation/growth balance, typically favoring faster crystal growth and potentially more defined morphologies), and mass transfer. As a matter of fact, variations in the solvent environment and temperature affect Zn²⁺-ligand interactions and supersaturation levels, thereby altering nucleation rates and particle growth pathways.





View Article Online
DOI: 10.1039/D5GC05937B

Figure 3. SEM micrographs of (a) sample 8 (b) sample 16 (c) sample 9 with a 100.00K magnification.

TEM was used to provide information on the primary particle size, complementing SEM analysis, which reflects aggregation and polydispersity. In agreement with SEM observations, all samples consist of nanostructured particles whose size depends on the solvent composition. In particular, ZIF-8 synthesized in pure DMC at room temperature exhibits particles of approximately 100 nm, whereas smaller nanocrystals are obtained in DMC/MeOH mixtures (Figure S12).

The solvent controls the growth and morphology of ZIF-8 crystals depending on the polarity, solubility, viscosity, and molecular structure of the solvent itself. Thus, the role of each solvent property is examined to obtain reasons of the differences between sample characterizations.

Pure DMC provides high interfacial tension between the dissolved reactants and the solvent so it creates a higher surface barrier to crystallization and retardation of the formation of nuclei. MeOH provides a lower interfacial tension than DMC, thereby creating a lower surface barrier against crystallization. It leads to accelerated crystallization, particularly increasing primary nuclei production. A large number of nuclei are created, and they grow to form ZIF-8 crystals. Thus, a higher product yield is obtained in the DMC/MeOH 2:1 mixture compared to pure MeOH, as shown in Tables 1 and 2. In addition, when the reaction mixture contains an excess of methanol (DMC/MeOH 1:2) and the solvent characteristics are thus more similar to pure methanol than to DMC, different reaction conditions are requested for this polar mixture. Considering the interfacial tension, DMC favors the formation of ZIF-8 at 25 °C rather than at 60 °C.

DMC shows a very weak polarity ($\epsilon \approx 3.1$) and is a non-protic solvent, but under the investigated reaction conditions, it allows the complete solubilization of both Hmim and zinc acetate. Using MeOH ($\epsilon \approx 32.6$), which increases the polarity of the solvent mixture compared to pure DMC, the reagents' solubility in the reaction media was enhanced. This, considering the polarity of ZIF-8 precursors, can result in a faster nucleation process in addition to a larger number of nuclei. This aspect, which may seem unavoidable, is the key that has been used to prepare ZIF-8 at 25°C in DMC.

Solvent viscosity is related to mass transfer, and mass transfer is a superior factor in the growth of ZIF-8 particles. Relying on the theory of diffusion-limited aggregation, diffusion limitation adjusts the chemical diffusion and reaction rates in the synthesized samples. Therefore, the diffusivity of reactants defines the crystal growth pathway. The diffusion of reactants is changed by using the different kinds of solvents, and for instance, the diffusivity of Zn^{2+} in MeOH is $0.544 \times 10^{-4} \text{ cm}^2 \text{ s}^{-1}$,¹⁶ whereas in DMC the calculated value using the Stokes–Einstein equation is $0.505 \times 10^{-4} \text{ cm}^2 \text{ s}^{-1}$. In this case, the diffusion of the reagents can be assumed substantially similar for pure DMC and the DMC/MeOH mixtures.

These considerations are further supported by information on the primary particle size (TEM images, Figure S12). ZIF-8 samples synthesized in pure DMC at room temperature exhibit larger particles



with respect to those in DMC/MeOH mixtures. This behavior is consistent with a solvent-dependent nucleation–growth mechanism. In low-polarity DMC, lower effective solvation, reduced availability of reactive species and higher interfacial barriers lead to slower nucleation and fewer nuclei, allowing crystal growth to dominate and resulting in larger particles. In contrast, the increased polarity in DMC/MeOH mixtures enhances precursor solubility and promotes a higher nucleation rate, generating a larger number of nuclei and consequently smaller particles.

In summary, we considered the influence of this parameter to be equal in our experiments. However, when considering the use of organic carbonates (OCs) as solvents for ZIF-8 preparation, we observed substantial differences compared to the results reported for GlyC, where a mesoporous ZIF-8 was obtained. A polar, protic, and viscous solvent such as GlyC favors the development of mesoporous ZIF-8 in contrast to a non-polar, aprotic, and low-viscosity solvent like DMC, where microporous ZIF-8 with higher specific surface area (1522 vs 660 m² g⁻¹ in GlyC in 24h) is obtained. The use of DMC enables the ZIF-8 preparation at 25 °C (100 °C is needed in GlyC) in only 1h, reducing the purification time due to its lower boiling point.

To further promote the use of DMC within a circular economy perspective, we carried out sequential ZIF-8 synthesis using recycled DMC over several cycles. The synthesis were performed under the same optimized conditions as those applied to the fresh solvent (entry 16 Table 3).

As reported in Table 4, the yields remained high across all cycles, with only a slight decrease from 91.3% in the first run with pure DMC to 85.5% after the third cycle. Similarly, BET SSA of samples 16-R1 and 16-R2 show comparable values, both higher than that of sample 16.

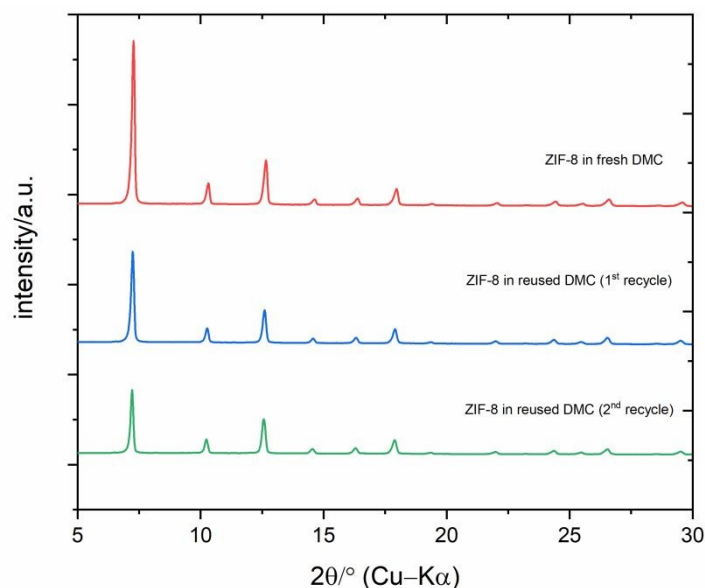
Table 4. ZIF-8 yield, BET specific surface areas and pore volume values for recycling tests.

Entry*	Solvent	Yield (%)	BET SSA (m ² g ⁻¹)	Total pore volume (cc g ⁻¹)
16-R1	Recovered DMC(x1)	88.0	1708	0.67
16-R2	Recovered DMC (x2)	85.5	1688	0.83

*ZIF-8 synthesised at 25°C for 1h ([Zn²⁺]/[Hmim]/ [NaOH] =5 mM/10 mM/10 mM).

ZIF-8 samples synthesized in recycled DMC retained the typical crystalline structure of ZIF-8, as confirmed by the XRPD diffraction patterns shown in Figure 12. Likewise, BET isotherms revealed the preservation of the same microporous features across all the synthesis cycles, and PSD curves confirmed the expected half-pore width of 0.588 nm (Figure S8 in SI).





View Article Online
DOI: 10.1039/D5GC05937B

Figure 4. XRPD diffraction patterns of ZIF-8 synthesized in fresh DMC (sample 16, red) and in recycled DMC (samples 16-R1, blue and 16-R2, green).

It's worth noticing that, according to literature, the reuse of mother liquors for ZIF-8 synthesis in MeOH may result in comparable or lower yields across several cycles, while surface area values generally vary within a narrow range.^{13,43} In this work, we achieved competitive results for both parameters even after multiple cycles. These findings further highlight the effectiveness and sustainability of DMC as a solvent, demonstrating its excellent recyclability and consistent performance across repeated synthesis cycles.

Mechanistic insights

To elucidate the role of the dimethyl carbonate (DMC) in modulating the stability of the ZIF-8 structural motifs, Density Functional Theory (DFT) calculations were performed using a simplified but chemically meaningful model of the real material. Specifically, the dimer consisting of the $Zn_2(mIm)_4$ unit was initially considered, where mIm is the deprotonated form of the Hmim ligand, generated in the presence of NaOH acting as a strong base. In this species, the deprotonated nitrogen atom coordinates as a σ -donor towards the Zn^{2+} metal centers, recapitulating the coordination motif characteristic of zeolitic imidazolate frameworks.

The thermodynamic stability of this dimeric unit was evaluated by calculating the formation energy, in terms of ΔG_{DMC} , with respect to the reactants $Zn(acac)_2 \cdot 2H_2O$ and mIm set as the zero energy. Solvent effects were accounted for by employing an implicit solvation model, treating the medium as a dielectric continuum with a dielectric constant of 3.1.

The results, reported in Scheme 3a, show that the formation of the $Zn_2(mIm)_4$ dimer is not thermodynamically favored, with a ΔG_{DMC} of 48.3 kcal/mol. Therefore, in the absence of further stabilizing effects, the dimer does not form.

Considering this result, we tried to explicitly include the role of the solvent. In particular, the coordination of the metal centers in the dimer was saturated by introducing explicit DMC molecules, forming the dimer $Zn_2(mIm)_4(DMC)_3$, in which the solvent coordinates to the Zn ions through the formation of dative bonds established between the oxygen of the carbonyl group of the DMC molecules and the d orbitals of the metals.

Despite saturation of the Zn^{2+} coordination sphere by explicit DMC molecules, the formation free energy of the $Zn_2(mIm)_4(DMC)_3$ dimer, computed with respect to the reactants $Zn(acac)_2 \cdot 2H_2O$,



mIm, and DMC at infinite distance, is not thermodynamically favored, with a ΔG_{DMC} of 30.6 kcal/mol (Scheme 3b). However, when compared to the $\text{Zn}_2(\text{mIm})_4$ dimer, the formation of the $\text{Zn}_2(\text{mIm})_4(\text{DMC})_3$ species is more favorable by approximately 18 kcal/mol.

Although this result highlights the possible stabilizing effect exerted by solvent coordination, such stabilization is not sufficient to reverse the overall thermodynamic trend, and the dimeric species remains disfavored under the considered conditions (compare ΔG_{DMC} in Scheme 3a and 3b).

Finally, to recall the local structural motif of ZIF-8, in which tetrahedral Zn^{2+} are connected by mIm ligands in an extended three-dimensional lattice, the three DMC molecules present in the $\text{Zn}_2(\text{mIm})_4(\text{DMC})_3$ model were replaced with three Hmim molecules, forming the dimeric unit $\text{Zn}_2(\text{mIm})_4(\text{Hmim})_3$ (Scheme 3c).

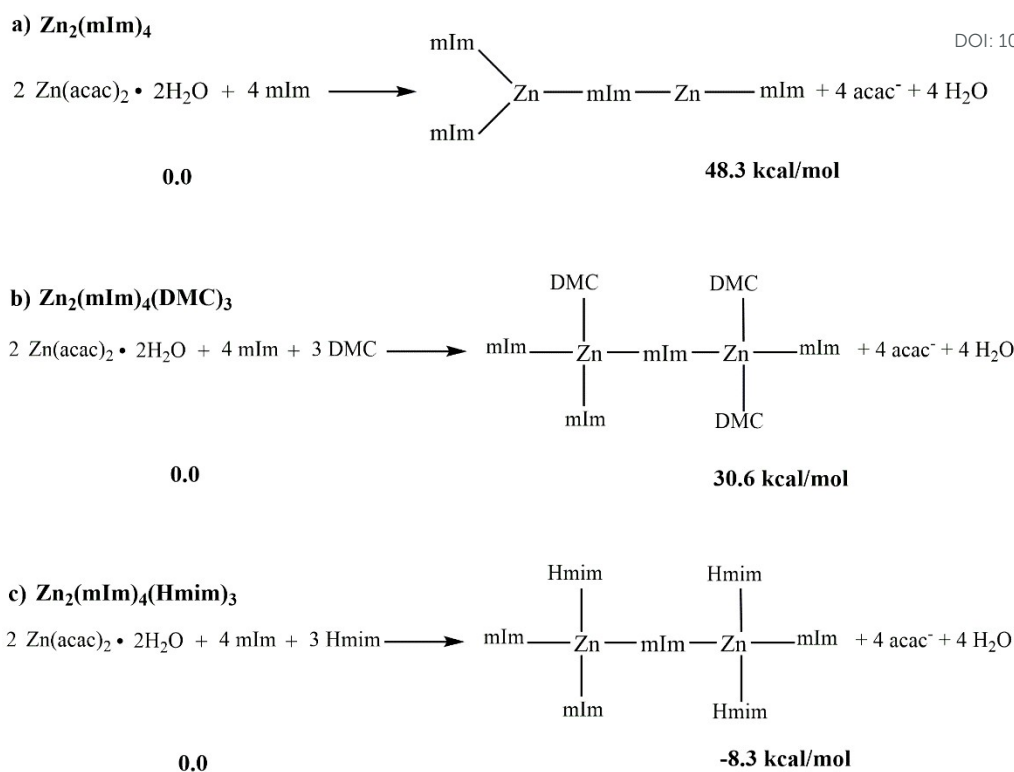
It is important to note that, in the infinite crystal of ZIF-8, each mIm acts as a bridge between two Zn^{2+} centers, and, therefore, each imidazole nitrogen atom is involved in metal coordination. When considering a finite model such as the $\text{Zn}_2(\text{mIm})_4$ dimer, dangling bonds, corresponding to sites where, in the real structure, an additional Zn^{2+} center would be present, are inevitably introduced. To this extent, we used hydrogen atoms on the ligands (Hmim) to saturate the site that, in the crystal, would instead be involved in coordination with another Zn^{2+} , minimizing the absence of the subsequent unit and avoiding the presence of non-physical charges or electronic states associated with incomplete bonds.

This more realistic representation of the system produces a change in the energy. In fact, the formation of the $\text{Zn}_2(\text{mIm})_4(\text{Hmim})_3$ dimer, computed with respect to the energy of $\text{Zn}(\text{acac})_2 \cdot 2\text{H}_2\text{O}$, mIm, and Hmim at infinite distance, results in a thermodynamically favored state with a ΔG_{DMC} of -8.3 kcal/mol (Scheme 3c). The growth of the ZIF repeating unit thus proceeds through Zn^{2+} centers that strictly adopt a tetrahedral geometry, featuring a coordination sphere of two anionic and two dative ligands. This configuration ensures a stable and energetically favorable pathway for framework propagation.

Overall, the role of the solvent is to modulate the strength and stability of the metal-ligand interactions.

The optimized structure of $\text{Zn}_2(\text{mIm})_4$, $\text{Zn}_2(\text{mIm})_4(\text{DMC})_3$ and $\text{Zn}_2(\text{mIm})_4(\text{Hmim})_3$ are reported in the Figure S11 of the SI.





Scheme 3. Formation mechanisms of the dimers a) $Zn_2(mIm)_4$, b) $Zn_2(mIm)_4(DMC)_3$ and c) $(Zn_2(mIm)_4(Hmim)_3)$ with the corresponding variation of free energies in DMC solvent (ΔG_{DMC} in kcal/mol).

Green metrics and simplified sustainability assessment

The greenness of the ZIF-8 synthesis in DMC was also evaluated through the application of green metrics, namely the simple E-factor (sEF) and Process Mass Intensity (PMI), providing a means to validate the adherence to Green Chemistry principles in terms of waste generation and mass-based process efficiency. sEF and PMI calculations are described in the Section S7.1 of the SI. This evaluation was carried out by comparing the results obtained in DMC with those reported in literature for several solvents (water, DMF, methanol and GlyC). In summary, DMC exhibited the lowest values -including recycling tests in the calculation (sEF= 0.8; PMI(r)= 2) - remarkably close to the ideal values of 0 and 1, respectively, thus outperforming conventional solvents, as detailed in Figure 5. Specifically, water shows the highest values for both sEF and PMI, followed by DMF and MeOH. GlyC also provides encouraging results, as extensively discussed in a recent work.²⁷

The highest values for DMF and H_2O can be reasonably attributed to the large excess of Hmim, while in the case of MeOH they can be associated with the relatively low ZIF-8 yields. It is evident that when the recycling of the reaction medium is considered, these values drastically decrease. In conclusion, these results clearly demonstrate the reduced environmental impact of our optimized process, achieved through high reaction yields under mild conditions and stoichiometric reagent ratios. This advantage is further strengthened by the excellent recyclability of DMC across consecutive synthesis cycles.



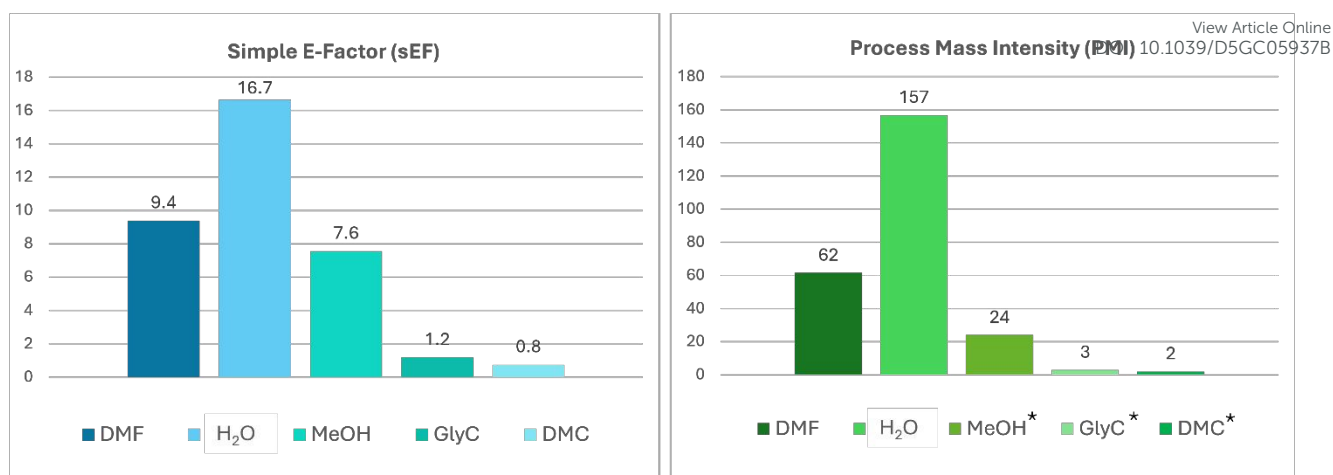


Figure 5. Comparison of simple E-Factor (left) and Process Mass Intensity (right) calculated for ZIF-8 synthesis in different solvents. *PMI(r).

At this stage, it is essential to integrate these mass-based metrics with those that assess the actual environmental impact of the process through the life cycle assessment (LCA) approach. Life Cycle Assessment (LCA) is a well-established and standardized methodology, governed by ISO 14040⁶¹ and 14044⁶², used to evaluate the potential environmental impacts of a product or process across its entire life cycle, from raw material extraction up to manufacturing and eventual disposal.

Within this framework, the optimized synthesis involving DMC was compared, in terms of environmental impacts, with the literature benchmark, namely the ZIF-8 synthesis using DMF as solvent.

For the setup of the LCA study, a comparative “cradle to gate” evaluation was performed adopting a functional unit (FU) as 1 g of ZIF-8. The software and database used, as well as the scenarios’ description and detailed life cycle inventory (LCI) of mass and energy fluxes are extensively described in the Section S7.2 of the SI.

The results of the comparison between the DMF-based scenario and the DMC-based scenario are presented in Figure 6. The assessment was carried out using both Midpoint and Endpoint indicators. In the first graph (a) all midpoint-level impacts values referring to DMF scenario are normalized to 100%, and the DMC-scenario impacts are reported as percentages. For most categories, DMC scenario scores are significantly lower, ranging approximately from a minimum of 42% to 78% relative to those of the DMF scenario. The endpoint-level results (b), expressed in mPts, reveal the same trend, namely the lower overall impacts of DMC scenario compared to the DMF ones. It’s noteworthy that, for both scenarios, the most affected category is that related to human health damage, mainly due to the significant electricity demand required to carry out the reactions.

Nevertheless, given the need to limit or replace the use of DMF because of its potential safety and human health risks, the DMC-based route represents a promising and more sustainable alternative for ZIF-8 synthesis.



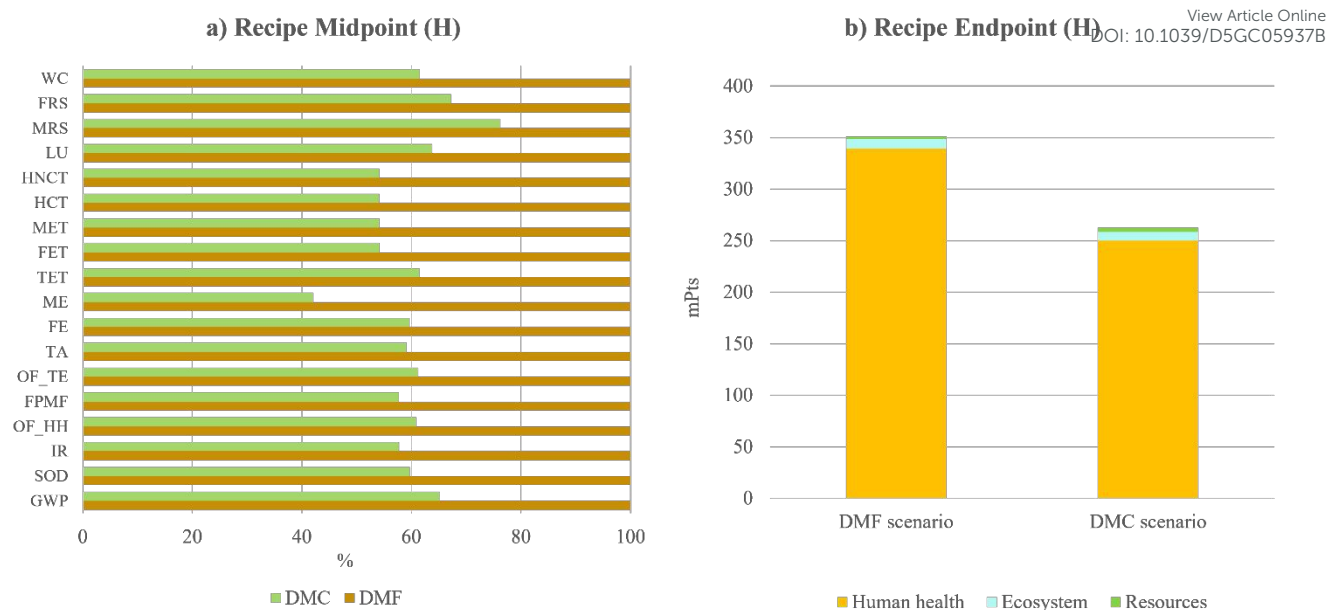


Figure 6. DMF and DMC based scenarios, compared in terms of a) midpoint and b) endpoint values (ReCiPe 2016 Midpoint (H) V1.07 / World (2010) H).

Conclusions

Microporous ZIF-8 was prepared with high yields (>90%) in DMC using only stoichiometric amounts of reagents, enlarging the choice of suitable organic solvents for this synthesis. In contrast to DMF, the most commonly used organic solvent for ZIF-8 preparation, the use of DMC favored the adoption of a recommended green solvent with non-significant toxicity.³⁶ Moreover, it was easily removed at the end of the synthesis, and the obtained ZIF-8 was readily purified by heating (as confirmed by TG analysis), in clear contrast with the limitations generally posed by other organic solvents. In DMC/MeOH waste-derived mixtures, we observed ZIF-8 with high yields up to 97.5% in 1h at 60 °C, comparable to the best results reported using conventional organic solvents. Furthermore, high specific surface areas were achieved within only 1h. DMC demonstrated excellent recyclability, enabling up to three consecutive synthesis cycles with negligible loss in yield and full preservation of ZIF-8 structural and textural properties. Moreover, the process exhibited green metrics remarkably close to the ideal values (sEF = 0.8; PMI(r)= 2), confirming the reduced environmental impact of DMC compared to other commonly used solvents for ZIF-8 preparation. LCA results, expressed both in terms of midpoint and endpoint indicators, further demonstrated that our method is characterized by lower environmental impacts than the synthesis carried out in DMF. The combination of high efficiency and enhanced sustainability makes the ZIF-8 synthesis in DMC a promising and viable route for achieving a mild-condition process with reduced environmental repercussions.

This work opens up new perspectives in the field of MOFs preparation and, in particular, to new synthetic procedures for ZIF-8 synthesis.

Acknowledgements

The authors sincerely thank Prof. Vincenzo Venditto, Prof. Vincenzo Vaiano and Pasqualmorica Antico for fruitful discussions and BET analyses. R.C. is grateful to University of Salerno for research fund “FARB” (ORSA234311) and to Italian Ministry of University and research (MUR) for FISA-2023- 00132 project “ALTEREGO - ALuminum wasTEs recYcling and valoRisation for Environmentally friendly GOals” - Area “Advanced Materials” (CUP D43C23004630001). I.L.



acknowledges the support provided by the HUN-REN Hungarian Research Network and the National Research, Development and Innovation Office of Hungary (K146071). New Article Online
DOI: 10.1039/D5GC05937B

References

- (1) Tan, J. C.; Bennett, T. D.; Cheetham, A. K. Chemical Structure, Network Topology, and Porosity Effects on the Mechanical Properties of Zeolitic Imidazolate Frameworks. *Proc. Natl. Acad. Sci. U.S.A.* **2010**, *107* (22), 9938–9943. <https://doi.org/10.1073/pnas.1003205107>.
- (2) Zheng, Z.; Rong, Z.; Nguyen, H. L.; Yaghi, O. M. Structural Chemistry of Zeolitic Imidazolate Frameworks. *Inorg. Chem.* **2023**, *62* (51), 20861–20873. <https://doi.org/10.1021/acs.inorgchem.3c02322>.
- (3) Kaneti, Y. V.; Dutta, S.; Hossain, Md. S. A.; Shiddiky, M. J. A.; Tung, K.; Shieh, F.; Tsung, C.; Wu, K. C. -W.; Yamauchi, Y. Strategies for Improving the Functionality of Zeolitic Imidazolate Frameworks: Tailoring Nanoarchitectures for Functional Applications. *Advanced Materials* **2017**, *29* (38), 1700213. <https://doi.org/10.1002/adma.201700213>.
- (4) Kouser, S.; Hezam, A.; Khadri, M. J. N.; Khanum, S. A. A Review on Zeolite Imidazole Frameworks: Synthesis, Properties, and Applications. *J Porous Mater* **2022**, *29* (3), 663–681. <https://doi.org/10.1007/s10934-021-01184-z>.
- (5) Bergaoui, M.; Khalfoui, M.; Awadallah-F, A.; Al-Muhtaseb, S. A Review of the Features and Applications of ZIF-8 and Its Derivatives for Separating CO₂ and Isomers of C₃- and C₄-Hydrocarbons. *Journal of Natural Gas Science and Engineering* **2021**, *96*, 104289. <https://doi.org/10.1016/j.jngse.2021.104289>.
- (6) Chen, B.; Yang, Z.; Zhu, Y.; Xia, Y. Zeolitic Imidazolate Framework Materials: Recent Progress in Synthesis and Applications. *J. Mater. Chem. A* **2014**, *2* (40), 16811–16831. <https://doi.org/10.1039/C4TA02984D>.
- (7) Bhattacharjee, S.; Jang, M.-S.; Kwon, H.-J.; Ahn, W.-S. Zeolitic Imidazolate Frameworks: Synthesis, Functionalization, and Catalytic/Adsorption Applications. *Catal Surv Asia* **2014**, *18* (4), 101–127. <https://doi.org/10.1007/s10563-014-9169-8>.
- (8) Matusiak, J.; Przekora, A.; Franus, W. Zeolites and Zeolite Imidazolate Frameworks on a Quest to Obtain the Ideal Biomaterial for Biomedical Applications: A Review. *Materials Today* **2023**, *67*, 495–517. <https://doi.org/10.1016/j.mattod.2023.06.008>.
- (9) Wang, T.; Wang, Y.; Sun, M.; Hanif, A.; Wu, H.; Gu, Q.; Ok, Y. S.; Tsang, D. C. W.; Li, J.; Yu, J.; Shang, J. Thermally Treated Zeolitic Imidazolate Framework-8 (ZIF-8) for Visible Light Photocatalytic Degradation of Gaseous Formaldehyde. *Chem. Sci.* **2020**, *11* (26), 6670–6681. <https://doi.org/10.1039/D0SC01397H>.
- (10) Kaur, H.; Mohanta, G. C.; Gupta, V.; Kukkar, D.; Tyagi, S. Synthesis and Characterization of ZIF-8 Nanoparticles for Controlled Release of 6-Mercaptopurine Drug. *Journal of Drug Delivery Science and Technology* **2017**, *41*, 106–112. <https://doi.org/10.1016/j.jddst.2017.07.004>.
- (11) Dai, H.; Yuan, X.; Jiang, L.; Wang, H.; Zhang, J.; Zhang, J.; Xiong, T. Recent Advances on ZIF-8 Composites for Adsorption and Photocatalytic Wastewater Pollutant Removal: Fabrication, Applications and Perspective. *Coordination Chemistry Reviews* **2021**, *441*, 213985. <https://doi.org/10.1016/j.ccr.2021.213985>.
- (12) Feng, S.; Zhang, X.; Shi, D.; Wang, Z. Zeolitic Imidazolate Framework-8 (ZIF-8) for Drug Delivery: A Critical Review. *Front. Chem. Sci. Eng.* **2021**, *15* (2), 221–237. <https://doi.org/10.1007/s11705-020-1927-8>.
- (13) Liang, Y.; Guo, J.; Zhang, H.; Brett, D. J. L.; Gadipelli, S. Superior Supercapacitor Performance with Tuneable 2D/3D Morphological Microporous Carbons of Zeolitic Imidazolate Frameworks Synthesized by Recycling Mother Liquors. *Chemical Engineering Journal* **2024**, *489*, 151190. <https://doi.org/10.1016/j.cej.2024.151190>.
- (14) Park, K. S.; Ni, Z.; Côté, A. P.; Choi, J. Y.; Huang, R.; Uribe-Romo, F. J.; Chae, H. K.; O’Keeffe, M.; Yaghi, O. M. Exceptional Chemical and Thermal Stability of Zeolitic



Imidazolate Frameworks. *Proc. Natl. Acad. Sci. U.S.A.* **2006**, *103* (27), 10186–10191. <https://doi.org/10.1073/pnas.0602439103>. View Article Online
DOI: 10.1039/D5GC05937B

- (15) Lee, Y.-R.; Jang, M.-S.; Cho, H.-Y.; Kwon, H.-J.; Kim, S.; Ahn, W.-S. ZIF-8: A Comparison of Synthesis Methods. *Chemical Engineering Journal* **2015**, *271*, 276–280. <https://doi.org/10.1016/j.cej.2015.02.094>.
- (16) Akhundzadeh Tezerjani, A.; Halladj, R.; Askari, S. Different View of Solvent Effect on the Synthesis Methods of Zeolitic Imidazolate Framework-8 to Tuning the Crystal Structure and Properties. *RSC Adv.* **2021**, *11* (32), 19914–19923. <https://doi.org/10.1039/D1RA02856A>.
- (17) Sherwood, J.; Albericio, F.; De La Torre, B. G. *N*, *N*-Dimethyl Formamide European Restriction Demands Solvent Substitution in Research and Development. *ChemSusChem* **2024**, *17* (8), e202301639. <https://doi.org/10.1002/cssc.202301639>.
- (18) Pan, Y.; Liu, Y.; Zeng, G.; Zhao, L.; Lai, Z. Rapid Synthesis of Zeolitic Imidazolate Framework-8 (ZIF-8) Nanocrystals in an Aqueous System. *Chem. Commun.* **2011**, *47* (7), 2071. <https://doi.org/10.1039/c0cc05002d>.
- (19) Malekmohammadi, M.; Fatemi, S.; Razavian, M.; Nouralishahi, A. A Comparative Study on ZIF-8 Synthesis in Aqueous and Methanolic Solutions: Effect of Temperature and Ligand Content. *Solid State Sciences* **2019**, *91*, 108–112. <https://doi.org/10.1016/j.solidstatesciences.2019.03.022>.
- (20) Gross, A. F.; Sherman, E.; Vajo, J. J. Aqueous Room Temperature Synthesis of Cobalt and Zinc Sodalite Zeolitic Imidazolate Frameworks. *Dalton Trans.* **2012**, *41* (18), 5458. <https://doi.org/10.1039/c2dt30174a>.
- (21) Saliba, D.; Ammar, M.; Rammal, M.; Al-Ghoul, M.; Hmadeh, M. Crystal Growth of ZIF-8, ZIF-67, and Their Mixed-Metal Derivatives. *J. Am. Chem. Soc.* **2018**, *140* (5), 1812–1823. <https://doi.org/10.1021/jacs.7b11589>.
- (22) Farkas, S.; Fonyi, M. S.; Holló, G.; Németh, N.; Valletti, N.; Kukovecz, Á.; Schuszter, G.; Rossi, F.; Lagzi, I. Periodic Precipitation of Zeolitic Imidazolate Frameworks in a Gelled Medium. *J. Phys. Chem. C* **2022**, *126* (22), 9580–9586. <https://doi.org/10.1021/acs.jpcc.2c02371>.
- (23) Németh, N.; Holló, G.; Schuszter, G.; Horváth, D.; Tóth, Á.; Rossi, F.; Lagzi, I. Application of a Chemical Clock in Material Design: Chemically Programmed Synthesis of Zeolitic Imidazole Framework-8. *Chem. Commun.* **2022**, *58* (38), 5777–5780. <https://doi.org/10.1039/D2CC01139E>.
- (24) Németh, N.; Holló, G.; Valletti, N.; Farkas, S.; Dúzs, B.; Kukovecz, Á.; Schuszter, G.; Szalai, I.; Rossi, F.; Lagzi, I. Synthesis of Zeolitic Imidazolate Framework-8 Using an Electric Field in a Gelled Medium. *Mater. Adv.* **2023**. <https://doi.org/10.1039/D3MA00690E>.
- (25) Németh, N.; Lawson, H. S.; Holló, G.; Valletti, N.; Rossi, F.; Schuszter, G.; Lagzi, I. Non-Autonomous Zinc–Methylimidazole Oscillator and the Formation of Layered Precipitation Structures in a Hydrogel. *Sci Rep* **2023**, *13* (1), 11029. <https://doi.org/10.1038/s41598-023-37954-9>.
- (26) Prete, P.; Trano, S.; Zaccagnini, P.; Fagiolari, L.; Amici, J.; Lamberti, A.; Proto, A.; Bella, F.; Cucciniello, R. Glycerol Carbonate and Solketal Carbonate as Circular Economy Bricks for Supercapacitors and Potassium Batteries. *ChemSusChem* **2024**, *17* (24), e202401636. <https://doi.org/10.1002/cssc.202401636>.
- (27) Itatani, M.; Németh, N.; Valletti, N.; Schuszter, G.; Prete, P.; Lo Nostro, P.; Cucciniello, R.; Rossi, F.; Lagzi, I. Synthesis of Zeolitic Imidazolate Framework-8 Using Glycerol Carbonate. *ACS Sustainable Chem. Eng.* **2023**, *11* (35), 13043–13049. <https://doi.org/10.1021/acssuschemeng.3c02876>.
- (28) Valletti, N.; Acar, M.; Cucciniello, R.; Magrini, C.; Budroni, M. A.; Tatini, D.; Proto, A.; Marchettini, N.; Lo Nostro, P.; Rossi, F. Glycerol Carbonate Structuring in Aqueous Solutions as Inferred from Mutual Diffusion Coefficient, Density and Viscosity Measurements in the



- Temperature Range 283.15–313.15 K. *Journal of Molecular Liquids* **2022**, *357*, 119114. <https://doi.org/10.1016/j.molliq.2022.119114>. New Article Online
DOI: 10.1039/D5GC05937B
- (29) León-Alcaide, L.; López-Cabrelles, J.; Esteve-Rochina, M.; Ortí, E.; Calbo, J.; Huisman, B. A. H.; Sessolo, M.; Waerenborgh, J. C.; Vieira, B. J. C.; Mínguez Espallargas, G. Implementing Mesoporosity in Zeolitic Imidazolate Frameworks through Clip-Off Chemistry in Heterometallic Iron–Zinc ZIF-8. *J. Am. Chem. Soc.* **2023**, *145* (42), 23249–23256. <https://doi.org/10.1021/jacs.3c08017>.
- (30) Cravillon, J.; Münzer, S.; Lohmeier, S.-J.; Feldhoff, A.; Huber, K.; Wiebcke, M. Rapid Room-Temperature Synthesis and Characterization of Nanocrystals of a Prototypical Zeolitic Imidazolate Framework. *Chem. Mater.* **2009**, *21* (8), 1410–1412. <https://doi.org/10.1021/cm900166h>.
- (31) Kida, K.; Okita, M.; Fujita, K.; Tanaka, S.; Miyake, Y. Formation of High Crystalline ZIF-8 in an Aqueous Solution. *CrystEngComm* **2013**, *15* (9), 1794. <https://doi.org/10.1039/c2ce26847g>.
- (32) Kim, Y. J.; Kim, M.-Z.; Alam, S. F.; Rehman, A. U.; Devipriyanka, A.; Sharma, P.; Lee, H. R.; Cho, C.-H. Polarity-Dependent Particle Size of Zeolitic Imidazolate Framework Synthesized in Various Solvents. *Materials Chemistry and Physics* **2021**, *259*, 124021. <https://doi.org/10.1016/j.matchemphys.2020.124021>.
- (33) Kim, D.; Park, J.; Park, J.; Jang, J.; Han, M.; Lim, S.; Ryu, D. Y.; You, J.; Zhu, W.; Yamauchi, Y.; Kim, J. Surfactant-Free, Size-Controllable, and Scalable Green Synthesis of ZIF-8 Particles with Narrow Size Distribution by Tuning Key Reaction Parameters in Water Solvent. *Small Methods* **2024**, *8* (12), 2400236. <https://doi.org/10.1002/smt.202400236>.
- (34) Zhang, B.; Zhang, J.; Liu, C.; Sang, X.; Peng, L.; Wu, T.; Han, B.; Yang, G. Solvent Determines the Formation and Properties of Metal-Organic Framework. *RSC Adv.* **2015**, *5*, 37691–37696. <https://doi.org/10.1039/C5RA02440D>.
- (35) Fiorani, G.; Perosa, A.; Selva, M. Dimethyl Carbonate: A Versatile Reagent for a Sustainable Valorization of Renewables. *Green Chem.* **2018**, *20* (2), 288–322. <https://doi.org/10.1039/C7GC02118F>.
- (36) Prat, D.; Wells, A.; Hayler, J.; Sneddon, H.; McElroy, C. R.; Abou-Shehada, S.; Dunn, P. J. CHEM21 Selection Guide of Classical- and Less Classical-Solvents. *Green Chem.* **2016**, *18* (1), 288–296. <https://doi.org/10.1039/C5GC01008J>.
- (37) Tundo, P.; Selva, M. The Chemistry of Dimethyl Carbonate. *Acc. Chem. Res.* **2002**, *35* (9), 706–716. <https://doi.org/10.1021/ar010076f>.
- (38) Pyo, S.-H.; Park, J. H.; Chang, T.-S.; Hatti-Kaul, R. Dimethyl Carbonate as a Green Chemical. *Current Opinion in Green and Sustainable Chemistry* **2017**, *5*, 61–66. <https://doi.org/10.1016/j.cogsc.2017.03.012>.
- (39) Errichiello, F.; Cucciniello, R.; Tomasini, M.; Falivene, L.; Gambuti, A.; Cassiano, C.; Forino, M. Efficient and Selective Extraction of Oleanolic Acid from Grape Pomace with Dimethyl Carbonate. *Green Chem.* **2024**, *26* (19), 10177–10188. <https://doi.org/10.1039/D4GC03624G>.
- (40) Guo, C.; Liu, X.; Wang, F.; Cao, Y.; Zheng, S.; He, G. Economic Analysis and Life Cycle Environmental Assessment of Imidazolium-Based Ionic Liquids for Separation of the Methanol/Dimethyl Carbonate Azeotrope. *ACS Sustainable Chem. Eng.* **2023**, *11* (28), 10482–10495. <https://doi.org/10.1021/acssuschemeng.3c02059>.
- (41) Sessa, A.; Rossi, E.; Prete, P.; Passarini, F.; Itatani, M.; Lagzi, I.; Lo Nostro, P.; Cespi, D.; Cucciniello, R. Life Cycle Assessment of Solvothermal ZIF-8 Synthesis: Is the Substitution of DMF with Glycerol Carbonate Environmentally Sustainable? *ChemSusChem*, <https://doi.org/10.1002/cssc.202502019R2>.
- (42) De Caro, P.; Bandres, M.; Urrutigoity, M.; Cecutti, C.; Thiebaud-Roux, S. Recent Progress in Synthesis of Glycerol Carbonate and Evaluation of Its Plasticizing Properties. *Front. Chem.* **2019**, *7*, 308. <https://doi.org/10.3389/fchem.2019.00308>.



- (43) Yang, X.; Song, T.; Su, T.; Hu, J.; Wu, S. Exploring the Influence of the Reused Methanol Solution for the Structure and Properties of the Synthesized ZIF-8. *Processes* **2022**, *10* (9), 1705. <https://doi.org/10.3390/pr10091705>.
- (44) He, M.; Yao, J.; Liu, Q.; Wang, K.; Chen, F.; Wang, H. Facile Synthesis of Zeolitic Imidazolate Framework-8 from a Concentrated Aqueous Solution. *Microporous and Mesoporous Materials* **2014**, *184*, 55–60. <https://doi.org/10.1016/j.micromeso.2013.10.003>.
- (45) Molina, M. A.; Rodríguez-Campa, J.; Flores-Borrell, R.; Blanco, R. M.; Sánchez-Sánchez, M. Sustainable Synthesis of Zeolitic Imidazolate Frameworks at Room Temperature in Water with Exact Zn/Linker Stoichiometry. *Nanomaterials* **2024**, *14* (4), 348. <https://doi.org/10.3390/nano14040348>.
- (46) Yao, J.; He, M.; Wang, K.; Chen, R.; Zhong, Z.; Wang, H. High-Yield Synthesis of Zeolitic Imidazolate Frameworks from Stoichiometric Metal and Ligand Precursor Aqueous Solutions at Room Temperature. *CrystEngComm* **2013**, *15* (18), 3601. <https://doi.org/10.1039/c3ce27093a>.
- (47) Parulkar, A.; Brunelli, N. A. High-Yield Synthesis of ZIF-8 Nanoparticles Using Stoichiometric Reactants in a Jet-Mixing Reactor. *Ind. Eng. Chem. Res.* **2017**, *56* (37), 10384–10392. <https://doi.org/10.1021/acs.iecr.7b02849>.
- (48) Balog, E.; Varga, G.; Kukovecz, Á.; Tóth, Á.; Horváth, D.; Lagzi, I.; Schusztér, G. Polymorph Selection of Zeolitic Imidazolate Frameworks via Kinetic and Thermodynamic Control. *Crystal Growth & Design* **2022**, *22* (7), 4268–4276. <https://doi.org/10.1021/acs.cgd.2c00265>.
- (49) Russel, W. W. The Adsorption of Gases and Vapors. Volume I: Physical Adsorption (Brunauer, Stephen). *J. Chem. Educ.* **1944**, *21* (1), 52. <https://doi.org/10.1021/ed021p52.1>.
- (50) Thommes, M.; Kaneko, K.; Neimark, A. V.; Olivier, J. P.; Rodríguez-Reinoso, F.; Rouquerol, J.; Sing, K. S. W. Physisorption of Gases, with Special Reference to the Evaluation of Surface Area and Pore Size Distribution (IUPAC Technical Report). *Pure and Applied Chemistry* **2015**, *87* (9–10), 1051–1069. <https://doi.org/10.1515/pac-2014-1117>.
- (51) Mojoudi, N.; Mirghaffari, N.; Soleimani, M.; Shariatmadari, H.; Belver, C.; Bedia, J. Phenol Adsorption on High Microporous Activated Carbons Prepared from Oily Sludge: Equilibrium, Kinetic and Thermodynamic Studies. *Sci Rep* **2019**, *9* (1), 19352. <https://doi.org/10.1038/s41598-019-55794-4>.
- (52) Ta, D. N.; Nguyen, H. K. D.; Trinh, B. X.; Le, Q. T. N.; Ta, H. N.; Nguyen, H. T. Preparation of nano-ZIF-8 in Methanol with High Yield. *Can J Chem Eng* **2018**, *96* (7), 1518–1531. <https://doi.org/10.1002/cjce.23155>.
- (53) Pauly, T. R.; Liu, Y.; Pinnavaia, T. J.; Billinge, S. J. L.; Rieker, T. P. Textural Mesoporosity and the Catalytic Activity of Mesoporous Molecular Sieves with Wormhole Framework Structures. *J. Am. Chem. Soc.* **1999**, *121* (38), 8835–8842. <https://doi.org/10.1021/ja991400t>.
- (54) Seetharaj, R.; Vandana, P. V.; Arya, P.; Mathew, S. Dependence of Solvents, pH, Molar Ratio and Temperature in Tuning Metal Organic Framework Architecture. *Arabian Journal of Chemistry* **2019**, *12* (3), 295–315. <https://doi.org/10.1016/j.arabjcc.2016.01.003>.
- (55) <https://www.ccdc.cam.ac.uk/Solutions/Software/Csd/>.
- (56) Yin, H.; Kim, H.; Choi, J.; Yip, A. C. K. Thermal Stability of ZIF-8 under Oxidative and Inert Environments: A Practical Perspective on Using ZIF-8 as a Catalyst Support. *Chemical Engineering Journal* **2015**, *278*, 293–300. <https://doi.org/10.1016/j.cej.2014.08.075>.
- (57) James, J. B.; Lin, Y. S. Kinetics of ZIF-8 Thermal Decomposition in Inert, Oxidizing, and Reducing Environments. *J. Phys. Chem. C* **2016**, *120* (26), 14015–14026. <https://doi.org/10.1021/acs.jpcc.6b01208>.
- (58) Missaoui, N.; Kahri, H.; Demirci, U. B. Rapid Room-Temperature Synthesis and Characterizations of High-Surface-Area Nanoparticles of Zeolitic Imidazolate Framework-8 (ZIF-8) for CO₂ and CH₄ Adsorption. *J Mater Sci* **2022**, *57* (34), 16245–16257. <https://doi.org/10.1007/s10853-022-07676-w>.



- (59) Troyano, J.; Carné-Sánchez, A.; Avci, C.; Imaz, I.; Maspoch, D. Colloidal Metal–Organic Framework Particles: The Pioneering Case of ZIF-8. *Chem. Soc. Rev.* **2019**, *48* (23), 5534–5546. <https://doi.org/10.1039/C9CS00472F>. View Article Online
DOI: 10.1039/C9GC05937B
- (60) Tsai, C.-W.; Langner, E. H. G. The Effect of Synthesis Temperature on the Particle Size of Nano-ZIF-8. *Microporous and Mesoporous Materials* **2016**, *221*, 8–13. <https://doi.org/10.1016/j.micromeso.2015.08.041>.
- (61) UNI EN ISO 14040:2006.
- (62) UNI EN ISO 14044:2006.



The authors confirm that the data supporting the findings of this study are available within the article [and/or] its supplementary materials.

View Article Online
DOI: 10.1039/D5GC05937B

